Chemistry, Physics and Technology of Surface. 2019. V. 10. N 4. P. 377-388

UDC 544.52+549.514.6+546.26 doi: 10.15407/hftp10.04.377

M.V. Shapovalova [1], T.A. Khalyavka [1], O.Y. Khyzhun [2], N.D. Shcherban [3], V.V. Permyakov [4], S.N. Scherbakov [5]

THE INFLUENCE OF TITANIUM DIOXIDE MODIFICATION BY SULFUR AND CARBON ON PHYSICO-CHEMICAL AND PHOTOCATALYTIC PROPERTIES

[1] Institute for Sorption and Problems of Endoecology of National Academy of Sciences of Ukraine
13 General Naumov Str., Kyiv, 03164, Ukraine, E-mail: takhalyavka@ukr.net
[2] Frantsevich Institute for Problems of Materials Science of National Academy of Sciences of Ukraine
3 Krzhizhanovsky Str., Kyiv, 03142, Ukraine
[3] L.V. Pisarzhevskii Institute of Physical Chemistry of National Academy of Sciences of Ukraine
31 Prospekt Nauky, Kyiv, 03028, Ukraine
[4] Institute of Geological Sciences of National Academy of Sciences of Ukraine
55b O. Gonchar Str., Kyiv, 01054, Ukraine
[5] M.G. Kholodny Institute of Botany of National Academy of Sciences of Ukraine
2 Tereshenkivska Str., Kyiv, 01601, Ukraine

The nanocomposites based on TiO_2 doped with sulfur (S/TiO_2), carbon (C/TiO_2), carbon and sulfur ($S/C/TiO_2$) have been obtained. The powders were characterized by XRD, XPS, BET, SEM, EDX, TEM and UV-VIS spectroscopy. EDX and XPS spectroscopies prove that titanium dioxide powder includes only Ti and O elements, composites C/TiO_2 include the elements Ti, O, C, composites S/TiO_2 - Ti, O, S and composites $C/S/TiO_2$ - Ti, O, C, and S.

XRD analysis revealed the phase of anatase in all composites, rutile phase appeared with increasing of sulfur amount in sulfur-containing powders. It has been found that the composites consist of roundish agglomerates in the range of 5–30 μm. Sulfur additives decrease grain growth of titanium dioxide particles from 14 to 9–10 nm in S/TiO_2 composites, carbon leads to increase in particle size from 14 to 19 nm, simultaneous modification of titanium dioxide by carbon and sulfur leads to the formation of particles with sizes of 7–8 nm.

Analysis of nitrogen sorption–desorption isotherms for all synthesized samples has shown the presence of a hysteresis loop which is the evidence for mesoporous structure of the powders. The isotherms correspond to type IV of IUPAC classification for mesoporous materials with H1 type for C/TiO_2 and H_2 type for S/TiO_2, and $C/S/TiO_2$ of hysteresis loop. The modification of TiO_2 by carbon and sulfur leads to increase of the specific surface area (of about 1.8 times in the case of C/TiO_2, about 3.3 times for S/TiO_2 and about 4.7 times for $C/S/TiO_2$), pore volume and decrease of pore radius compared with TiO_2.

Absorption spectra of the nanocomposites showed a bathochromic shift as compared with the absorption band of pure TiO_2. It has been found that modification leads to band gap narrowing. Nanocomposite samples showed higher photocatalytic activity in the destruction of safranine T under UV and visible irradiation compared to pure TiO_2. It may be related to the participation of dopants in the inhibition of electron-hole recombination, prolongation of charges lifetime, increasing efficiency of interfacial charge separation and formation of doping electronic states.

***Keywords**: nanocomposites, titanium dioxide, carbon, sulfur, safranine T, photocatalytic activity*

INTRODUCTION

Titanium dioxide is widely used in photocatalysis, in particular, for destruction of organic and inorganic pollutants. However, it has several serious disadvantages: an insufficiently high quantum yield of the reaction, wide band gap (3.2 eV), high rate of electron-hole recombination, and peculiarity of light adsorption by TiO_2 resulting in its photochemical activity only in the UV region of spectrum. So, an urgent problem in photocatalysis is a search for photocatalysts active under visible light irradiation. Researchers are trying in many ways to extend the photoactivation TiO_2 wavelength in the visible region of the spectrum, which will increase the use of solar energy and prevent recombination of the electron-hole pairs and thus allow more charge carriers to successfully diffuse to the surface. One of the ways is modification of titanium dioxide with different additives [1–6].

Currently researchers are concentrated on non-metals as dopants due to their advantages.

Non-metals anions have impurity states located near valence band edge. A great interest was attracted to doping titanium dioxide with C [1, 4, 5, 7–10] and S [11–13] using different methods.

These authors have reported that such doping leads to an appearance the photocatalytic activity under visible light due to incorporated S or C atoms into the lattice of titanium dioxide and thus causes the generation of intermediate energy level in TiO_2, located above valence band, narrowing the energy gaps of TiO_2 and shifting the optical absorption from UV region to visible one. So, the modification of titanium dioxide with non-metals can be an effective way to improve the photocatalytic activity under visible irradiation.

Considering the above, the aim of our work was to determine and compare the effect of titanium dioxide modification with different amount of sulfur and carbon on the physicochemical and photocatalytic properties of these composites.

EXPERIMENTAL

Preparation of composites. Nanocomposite samples of titanium dioxide doped with carbon and sulfur were obtained by sol–gel procedure using titanium(IV) – ethylate (Aldrich), citric acid (Alfa Aesar), glycerol (Alfa Aesar), carbon and thiourea (Chempack) additives. Carbon was obtained according to technique developed in the Institute for Sorption and Problems of Endoecology NAS of Ukraine [14]. The powders were prepared at stepwise heating (200, 300, 400 and 500 °C) in the presence of air. The samples were labeled as $1C/TiO_2$, $2C/TiO_2$, $3C/TiO_2$, $4C/TiO_2$ (the amount of carbon: 1, 1.5, 17, 21 wt. %, respectively); $1S/TiO_2$, $2S/TiO_2$, $3S/TiO_2$, $4S/TiO_2$ (the amount of sulfur: 2, 3, 13, 17.15 wt. %, respectively); $1S/C/TiO_2$, $2S/C/TiO_2$, $3S/C/TiO_2$, $4S/C/TiO_2$, $5/C/TiO_2$, $6S/C/TiO_2$, $7S/C/TiO_2$, (the content of sulfur: 0.6, 1.3, 2, 9, 12, 15 wt. %, respectively). For pure titanium dioxide, the same mixture (titanium(IV) – ethylate, citric acid, glycerol) was used, but without additives of carbon and thiourea.

Characterization of photocatalysts. Phase composition of the samples was determined by X-ray powder diffraction. A computerized Bruker D8 Advance diffractometer was equipped with CuK_α ($\lambda = 0.15406$ nm) X-ray source. All XRD peaks were checked and assigned to known crystalline phases. Average crystallite size was determined using broadening of the most intensive reflex using the Debye–Scherrer equation. Interplanar distance (d, nm) was calculated using Wulff–Bragg's equation.

Diffuse reflectance spectra (DRS) of the powders were measured using a Perkin-Elmer Lambda Bio 35 spectrophotometer in the range between 200 and 1000 nm which allows converting data of corresponding spectra using the Kubelka–Munk equation. The value of E_g was estimated by the method proposed by Wood and Tauc by the extrapolation of the linear part of the plot $(h\nu^*\alpha(h\nu))1/n$ versus $h\nu$ toward energy axis at $\alpha(h\nu) = 0$ (n = ½ for direct allowed transitions). The absolute and relative errors were ±0.01 eV and ±0.3 %, respectively.

To analyze sample composition (elemental analysis) and its morphology a scanning electron microscope (SEM JSM 6490 LV, JEOL, Japan) with an integrated system for electron microprobe analysis INCA. Energy based on energy-dispersive and wavelength-dispersive spectrometers (EDS + WDS, OXFORD, United Kingdom) with HKL Channel system was used.

Transmission electron microscopy (TEM) for received materials was carried out on a transmission electron microscope JEM-1200 EX (JEOL, Japan).

The values of the specific surface area (S_{sp}) of the samples as well as pore size distribution were determined using a Quantachrom NovaWin 2 device. The specific surface area of the samples was obtained from isotherms of nitrogen adsorption-desorption using the Brunauer–Emmet–Teller (BET) approach. The pore radius (R) and the pore volume (V_{tot}) were calculated from the desorption branches of the isotherms using the Barret–Joiner–Halenda method.

Presence of chemical elements and chemical bonds features in the samples were analyzed using X-ray photoelectron spectroscopy (XPS) on an UHV-Analysis-System equipment produced by SPECS Surface Nano Analysis Company (Berlin, Germany). The instrument was equipped with a semi-spherical analyzer PHOIBOS 150.

XPS spectra of core-level and valence electrons were analyzed in an UHV-Analysis-System chamber under residual pressure not higher than 7×10^{-8} Pa. XPS-spectra were

activated by X-ray MgK_α-irradiation (E = 1253.6 eV) and recorded at a constant pass energy of 30 eV. The energy scale of the device was graded by method [15] using reference metals Au and Cu. Surface charge of the samples was taken into account in reference to the energy of the C1*s*-line from hydrocarbon adsorbates which was set to 284.6 eV as recommended for transition metal oxides [16, 17].

Photocatalytic experiment. Photocatalytic activity of the samples was evaluated by the change of the concentration of safranine T (ST) (c = 0.03 g L^{-1}). Before irradiation, the catalyst suspension (2 g L^{-1}) in an aqueous solution of ST was kept in dark up to achieve adsorption equilibrium. The time to reach the adsorption equilibrium in the system powder – ST does not exceed 2 h for all the samples.

Irradiation of aqueous solutions (pH–6.5) of dye was performed at room temperature in a quartz reactor in the presence of air. The light source was a high-intensity Na discharge lamp GE Lucalox with power of 70 W, the latter emitting in the visible region with maxima at 568, 590 and 600 nm and an UV lamp BUV-30 with the power of 30 W and radiation maximum at 254 nm.

Concentrations of the ST were measured spectrophotometrically using a Shimadzu UV-2450 spectrophotometer at λ = 520 nm for ST. Photocatalytic rate constants for the model compound were calculated using the pseudofirst order kinetic equation.

RESULTS AND DISCUSSION

Investigation of the obtained powders by energy-dispersive spectroscopy based on energy-dispersive technique (Fig. 1) proves that TiO_2 powder includes only Ti and O elements, composites C/TiO_2 include the elements Ti, O, C, composites S/TiO_2 - Ti, O, S and composites $C/S/TiO_2$ - Ti, O, C and S.

Analysis of SEM-images of the samples shows randomly distributed agglomerates in the range of 5–30 μm (Fig. 1). The crystallite size in the agglomerates of the samples was calculated through Debye–Scherrer equation. The agglomerates of titanium dioxide consist of the particles of 14 nm in size. Modification with carbon leads to an increase in particle size: as the amount of carbon increases from 1 to 21 wt. %, the particle size increases from 14 to 19 nm. Sulfur additives inhibit grain growth of TiO_2 and form the particles of 9–10 nm in S/TiO_2 composites. Simultaneous modification of TiO_2 with carbon and sulfur leads to the formation of particles with a size of 7–8 nm. The change of TiO_2 particle sizes due to the doping with carbon and sulfur was confirmed by the TEM study (Fig. 2).

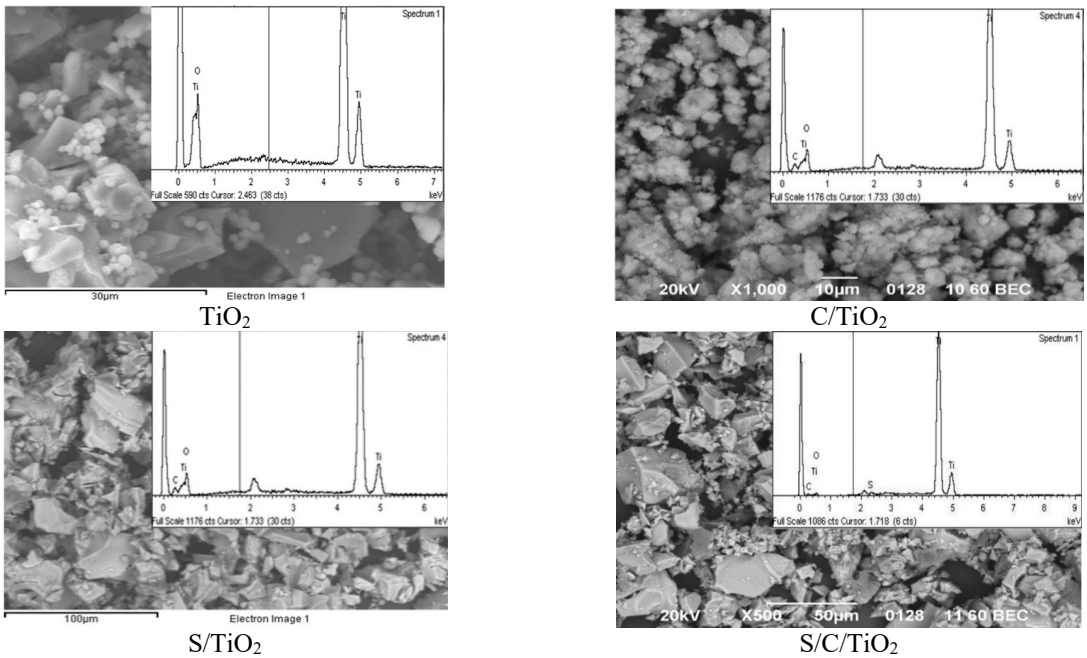

TiO_2 C/TiO_2

S/TiO_2 $S/C/TiO_2$

Fig. 1. SEM-images and EDS spectra of the samples

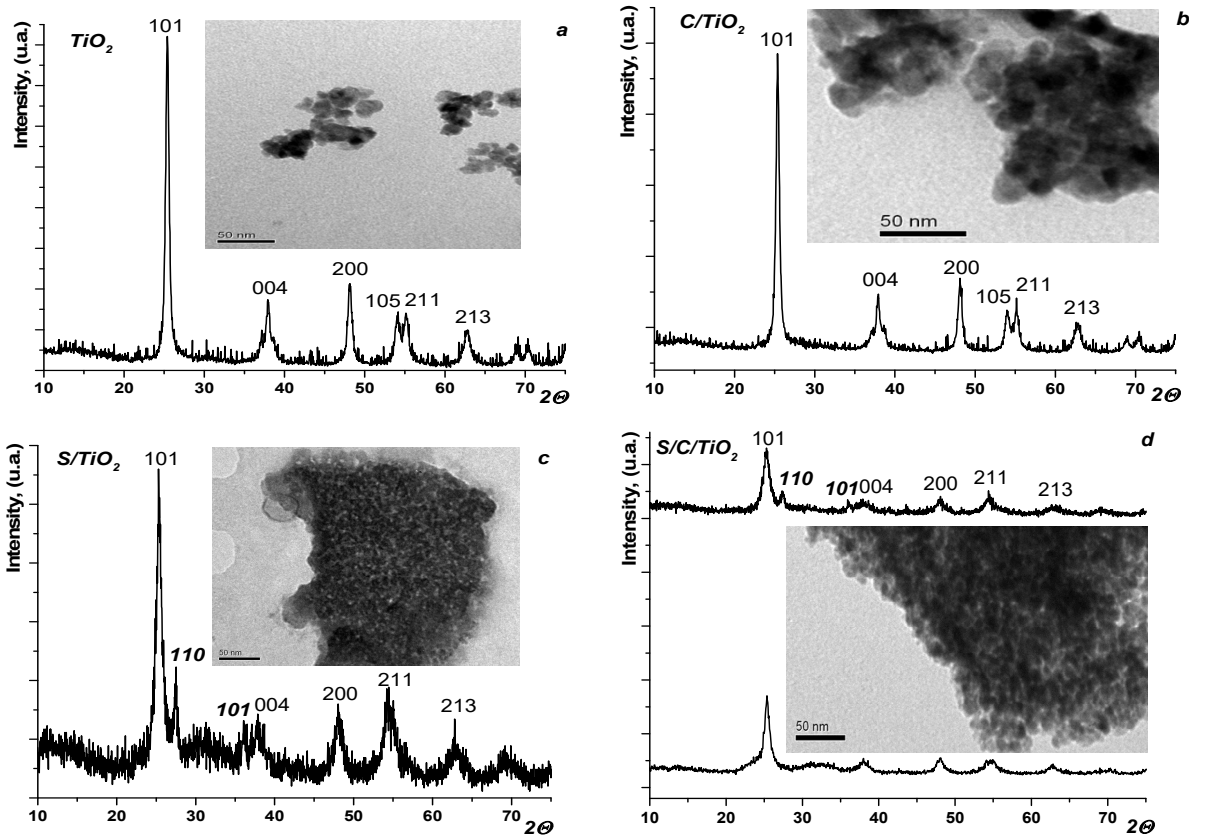

Fig. 2. XRD patterns and TEM-images of the samples

XRD pattern of pure titanium dioxide shows the reflexes of tetragonal modification of TiO_2 at $2\theta = 25.4$, 37.8, 48.0, 54.1, 55.0, 62.8 ° (Fig. 2), which correspond to the (101), (004), (200), (105), (211), (213) planes, respectively, and belong to the anatase phase (Fig. 2 *a*). All composites also show intensive peaks corresponding to the anatase phase (Fig. 2). No signal of brookite was detected. The peaks are quite broad, indicating small crystallite sizes. In contradiction to [2], additives of carbon into the binary composites do not induce new crystalline forms different from anatase (Fig. 2 *b*), which corresponds to the papers [5, 7, 8, 12]. In the case of S/TiO_2 (Fig. 2 *c*), XRD patterns show the reflexes of anatase ((101), (004), (200), (105), (211), (213)) and rutile ((110), (101)) phases regardless of sulfur concentration.

The addition of carbon (1.5 wt. %) and sulfur (from 0.6 to 9 wt. %) into ternary composites practically does not influence on the TiO_2 XRD pattern view (all reflexes of anatase are present) (Fig. 2 *d*, curve 1), which corresponds to the data obtained in preparation of nanocomposite by other methods [12, 18, 19]. But an increase in sulfur amount (12 and 15 wt. %) in the samples leads to appearance of new reflexes at $2\Theta = 27.4$ and 36.2 ° (Fig. 2 *d*, curve 2). It corresponds to the (110) and (101) planes of rutile. Thus, an increase of the sulfur amount in the ternary samples leads to the formation of rutile structure.

All composites show the presence of a hysteresis loop which is the evidence for mesoporous structure of the powders (Fig. 3). The isotherms correspond to type IV of IUPAC classification for mesoporous materials with H1 type for C/TiO_2 (Fig. 3 *a*) and H2 type for S/TiO_2 (Fig. 3 *b*) and $C/S/TiO_2$ (Fig. 3 *c*) of a hysteresis loop.

Predominance of pores up to 3.5 nm is characteristic of pure titanium dioxide, whereas the modification leads to a decrease in an average pore radius up to 2.5 nm for C/TiO_2 and to 1.7–2.4 nm for S/TiO_2. The ternary composites also have narrow pore size distribution – from 1.5 to 2.5 nm for samples with 0.6 to 9 wt. % of sulfur. Higher sulfur content (12 and 15 wt. %) in $C/S/TiO_2$ powders results in a larger pore size and broader pore size distribution (up to 3.5 nm). Similar results were obtained in [12].

It has been found that the surface area of composites depends on the dopant amount. The value of the specific surface area is increased of about 1.8 times in the case of C/TiO_2 (35–53 m^2/g), about 3.3 times for S/TiO_2 (60–95 m^2/g) and about 4.7 times for $C/S/TiO_2$ (80–133 m^2/g) as compared with that of titanium dioxide (28 m^2/g). These results are in accordance with the XRD, because the modification of titanium dioxide with carbon and sulfur leads to a decrease in the crystallite size and to an increase in the specific surface area of the samples.

Modification of titanium dioxide with carbon or sulfur in the case of binary and ternary composites leads to an increase in pore volume (for C/TiO_2 to 0.08, for S/TiO_2 – 0.21, for $C/S/TiO_2$ – 0.17) compared to TiO_2 (0.05 cm^3/g) and the radius decrease (for C/TiO_2 to 3.0, for S/TiO_2 – 2.1, for $C/S/TiO_2$ – 2.03 nm) compared to that of TiO_2 (3.8 nm).

The XPS spectra also prove that the composites include Ti, O, C and S (Fig. 4).

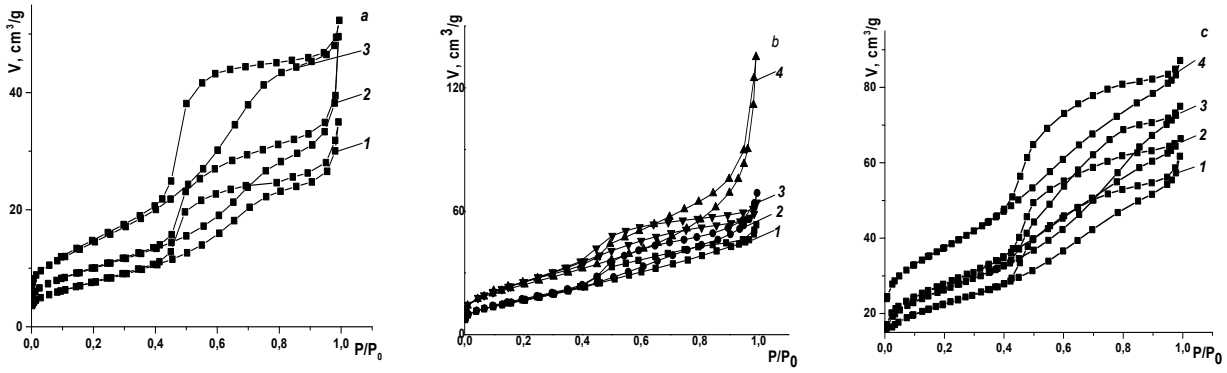

Fig. 3. Nitrogen adsorption–desorption isotherms of: (*a*) – TiO_2 (*1*), $1C1/TiO_2$ (*2*), $2C/TiO_2$ (*3*), (*b*) – $1S/TiO_2$ (*1*), $2S/TiO_2$ (*2*), $3S/TiO_2$ (*3*), $4S/TiO_2$ (*4*), (*c*) – $1S/C/TiO_2$ (*1*), $2S/C/TiO_2$ (*2*), $3S/C/TiO_2$ (*3*), $4S/C/TiO_2$ (*4*)

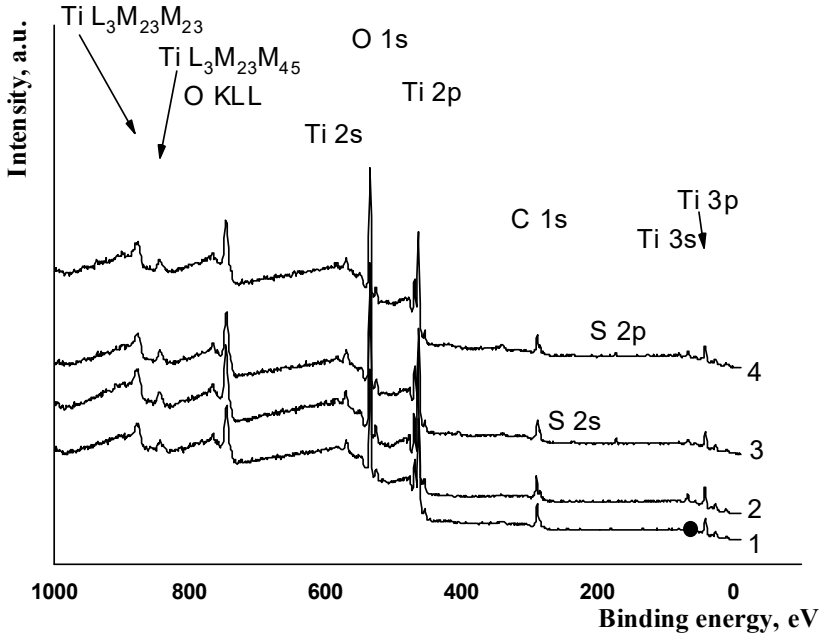

Fig. 4. XPS spectra of TiO_2 (*1*), $S/C/TiO_2$ (*2*), S/TiO_2 (*3*), C/TiO_2 (*4*)

The features of the XPS spectra in all the samples can be attributed to the core-level electronic levels of titanium, oxygen and carbon atoms, and the presence of sulfur is detected for S/TiO_2 and $C/S/TiO_2$ composites. Modification of titanium dioxide with sulfur and carbon does not lead to the appearance of some fine-structure features or to change in the energy position of the XPS spectra of core-level electrons (Table).

It has been previously reported [20] that a sulfur-containing material shows a binding energy value of around 170 eV. In our samples the presence of sulfur was confirmed by a peak at 168.4 eV (Fig. 4, 5 *a*). This peak is due to the presence of the SO_4^{2-} anion [21, 22]. In all S/TiO_2 and $C/S/TiO_2$ composites a peak at 168.4 eV was visible (Fig. 4, 5 *a*). Binding energy of S2*p*-electrons in composites S/TiO_2 and $C/S/TiO_2$ (Table, Fig. 5 *a*) corresponds to that for sulfur atoms in the compounds Na_2SO_4 and $FeSO_4$ [23].

Table. Binding energies of core-level electrons (±0.1 eV) of atoms constituting the investigated samples

Core level	Sample			
	TiO_2	$S/C/TiO_2$	S/TiO_2	C/TiO_2
O 2s	22.0	21.9	21.9	21.9
Ti 3p	36.9	37.0	36.9	37.0
S 2p	–	168.70	168.6	–
Ti $2p_{3/2}$	458.6	458.5	458.5	458.5
Ti $2p_{1/2}$	464.3	464.3	464.2	464.3
O 1s	530.0	530.0	530.0	529.9

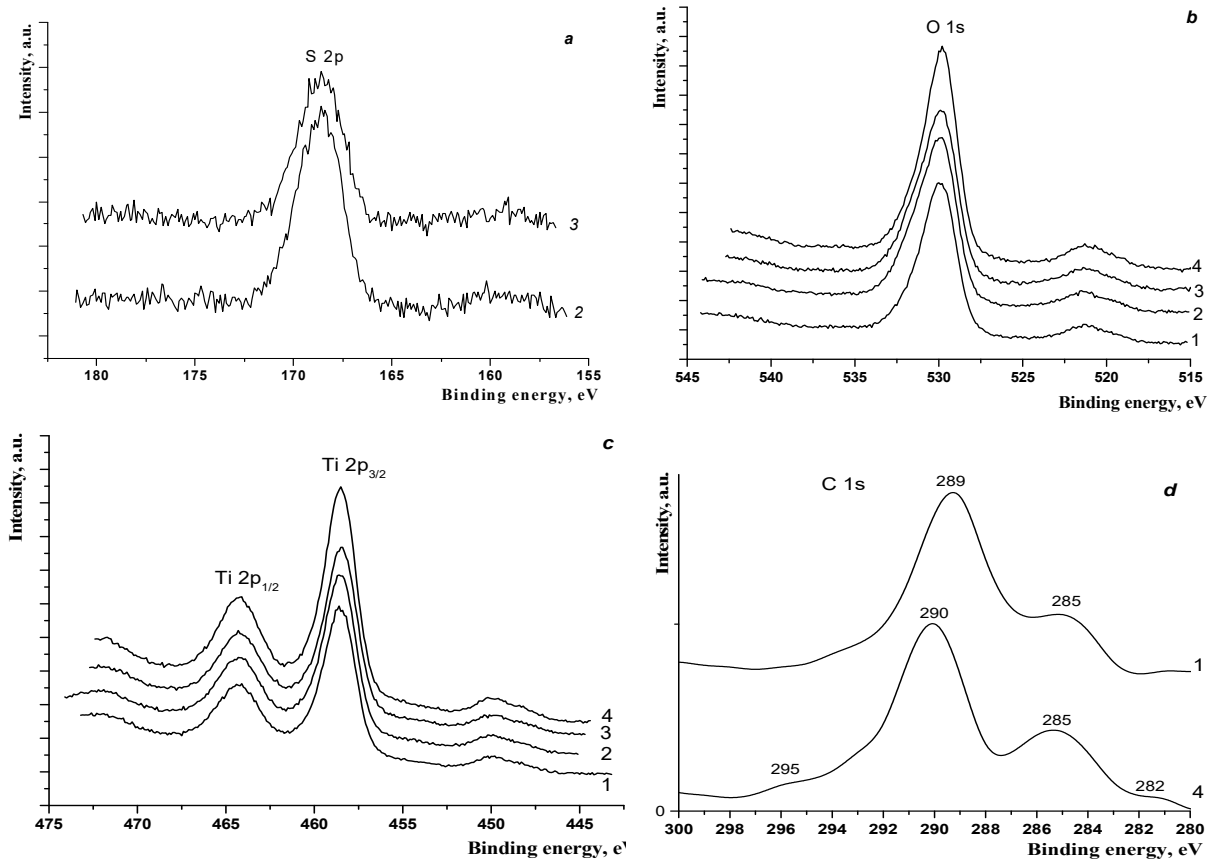

Fig. 5. XPS spectra of core-level S2*p* (*a*), O1*s* (*b*), and Ti2*p* (*c*) electrons and valence electrons (*d*) of TiO_2 (*1*), $S/C/TiO_2$ (*2*), S/TiO_2 (*3*), C/TiO_2 (*4*)

Energy positions of the XPS spectra of core-level Ti2$p_{3/2}$- and O1*s*-electrons (Table, Fig. 5 *b*, *c*) in the investigated samples are in a good agreement with the literature data regarding the values of binding energies of Ti 2$p_{3/2}$- and O1*s*- electrons in TiO_2 (458.5–459.0 eV for Ti2$p_{3/2}$-electrons and about 530 eV for O1*s*-electrons [23]).

It can be seen from Fig. 5 *d* that C 1s spectra at 295 to 282 eV can be observed. These species can be assigned to adventitious carbon species on the catalyst surface [24, 25]. The peak (about 285 eV) is thought to signal the presence of adventitious elemental carbon and the peak (289–290 eV) indicates the presence of C-O bonds [24–26] which are in agreement with our previous results on the C/TiO_2 composite FT-IR spectrum [27]. These peaks are more intensive for C/TiO_2 composite. There is a peak at about 282 eV for C/TiO_2 powder and it can be ascribed to carbon substituting for oxygen atom in the lattice of TiO_2, which resulted in formation of O–Ti–C bonds [24, 28]. The formation of carbonate species could cause an obvious long-tail absorption in the visible region [28]. Indeed, doping of titanium dioxide with carbon and sulfur leads to an appearance of a bathochromic shift as compared to the absorption band of pure TiO_2, the composite samples extended the absorption to the visible range (around 430 nm) (Fig. 6 *a*, *c*, *e*). Binary and ternary composites have absorption in the entire visible region in the form of a broad, unstructured band without expressed absorption maxima. This absorption can be divided into two parts: shoulder at about 400–430 nm and tail from 430 nm and further.

Also, modification of titanium dioxide with carbon leads to the narrowing of the band gap of the composites from 3.39±0.01 to 3.26±0.01 eV, doping of sulfur – from 3.25±0.01 to 3.04±0.01 eV, additives of carbon and sulfur – from 3.25±0.01 to 3.14±0.01 eV which contributes to reduce the energy required for photoactivation (Fig. 6 *b*, *d*, *f*). The bathochromic shift of the long-wavelength edge of the absorption band for the samples and the narrowing of the band gap occur because a part of the oxygen (lattice) atoms forming the valence band of TiO_2 are replaced by carbon atoms (Fig. 5 *d*). The appearance of absorption in the range of 3.12–3.14 eV for C/TiO_2 was observed and related to the formation of impurity (defect) levels in the band gap of TiO_2 upon carbon doping; that leads to sensitizing of C/TiO_2 composites to irradiation in the visible region of spectrum [10, 29].

The photocatalytic activity of all the materials was tested for destruction of safranine T in aqueous solution under UV and visible irradiation. Prior to irradiation, photocatalyst-dye systems were kept in the dark to achieve a sorption equilibrium. The adsorption–desorption equilibrium was achieved within 120 min. The sorption value of the dye on composites C/TiO_2 was 55–75 %, S/TiO_2 – 25–35 %, and $S/C/TiO_2$ – 60–80 %.

It is known that the dye molecules are capable to absorb UV light following their chemical transformations. The irradiation of safranine T solution without a photocatalyst shows that a negligible amount of dye molecules undergo photolysis under UV light (Fig. 7 *a*). The process of degradation of the dye is accelerated in the presence of powders (Fig. 7 *a*).

During the irradiation of safranine T with visible light (in the absence and in the presence of titanium dioxide), the destruction of the dye did not occur (Fig. 7 *b*). When the dye water solutions were irradiated with visible light in the presence of the composites, a decrease of ST concentrations was observed. The rate of process under UV and visible irradiation was dependent on catalyst composition and structure.

The composite samples showed higher photocatalytic activity in the decomposition of SF than pure titanium dioxide under UV and visible light (Fig. 7).

Experimental results have revealed that the rate of photocatalytic destruction of dye under UV and visible irradiation depends on dopants content. So, for C/TiO_2 sample the highest activity was detected with 1.5 wt. % of carbon. For ternary composites the rate is increased with an increase of sulfur content in the range of 0.6 to 1.3 wt. % and for S/TiO_2 of 2 to 17 wt. %. The sample $S/C/TiO_2$ with 1.3 wt. % of sulfur and the sample S/TiO_2 with 17 wt. % of sulfur possess the highest photocatalytic activity both under UV and visible irradiation (Fig. 7). Besides, these samples also showed the highest adsorption activity regarding safranine T. This indicates that, first of all, adsorbed molecules undergo photodestruction.

The enhanced UV and visible photocatalytic activity of nanocomposites is related to the participation of carbon in the inhibition of the recombination of photogenerated electrons and

holes due to efficient phase separation of charge [5]. The high photocatalytic activity of the composites upon irradiation by visible light may be attributed to the formation of additional energy levels in the band gap of TiO_2, which also leads to sensitization to visible light [12, 30].

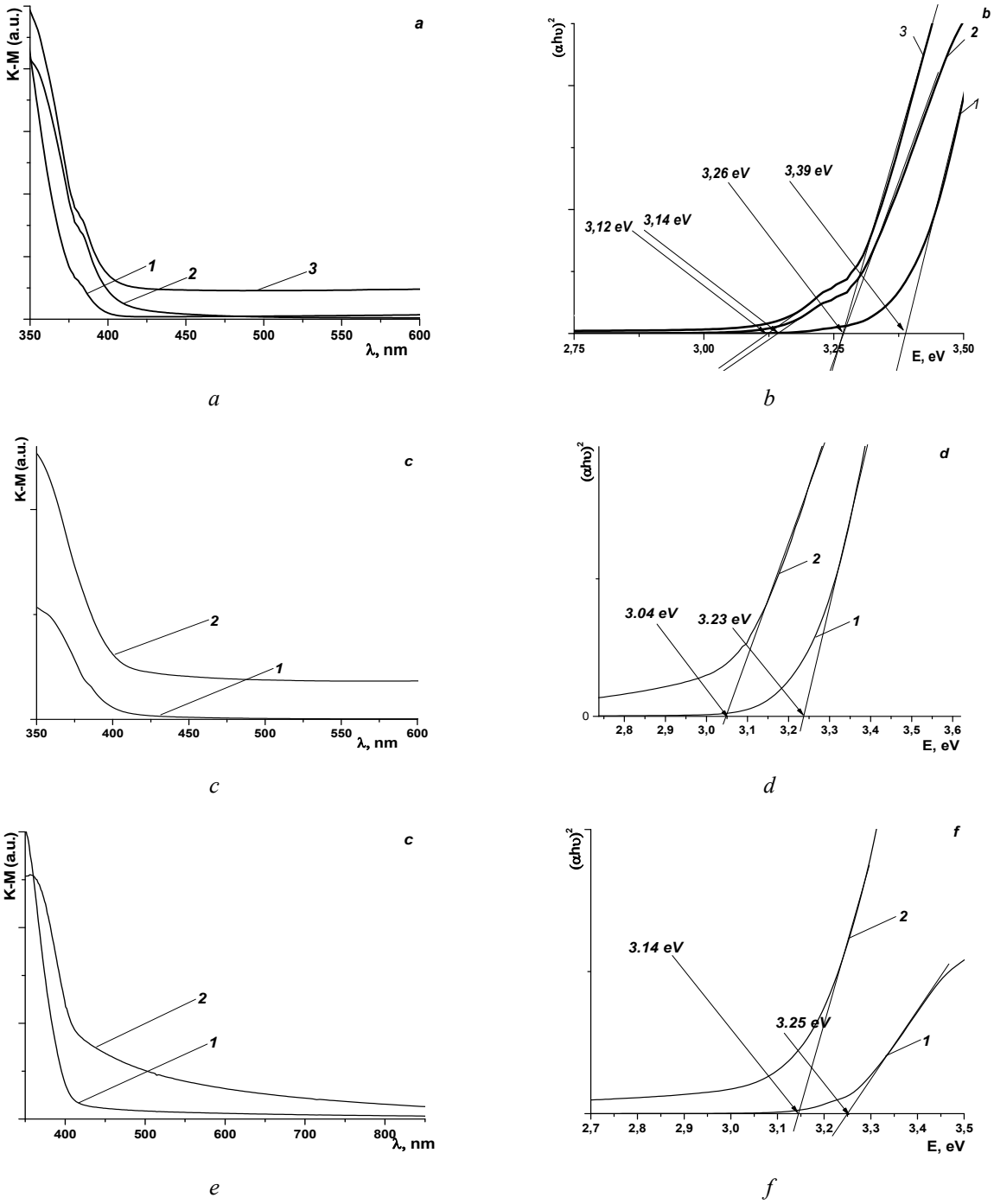

Fig. 6. DRS spectra (*a*, *c*, *e*) and corresponding plots of $(\alpha h\nu)^2$ (*b*, *d*, *f*) *versus* $h\nu$ of: (*a*, *b*) – TiO_2 (*1*), 1C/TiO_2 (*2*), 2C/TiO_2 (*3*), (*c*, *d*) – TiO_2 (*1*), 4S/TiO_2 (*2*), (*e*, *f*) – TiO_2 (*1*), 1S/C/TiO_2 (*2*), 2S/C/TiO_2 (*3*), 4S/C/TiO_2 (*4*)

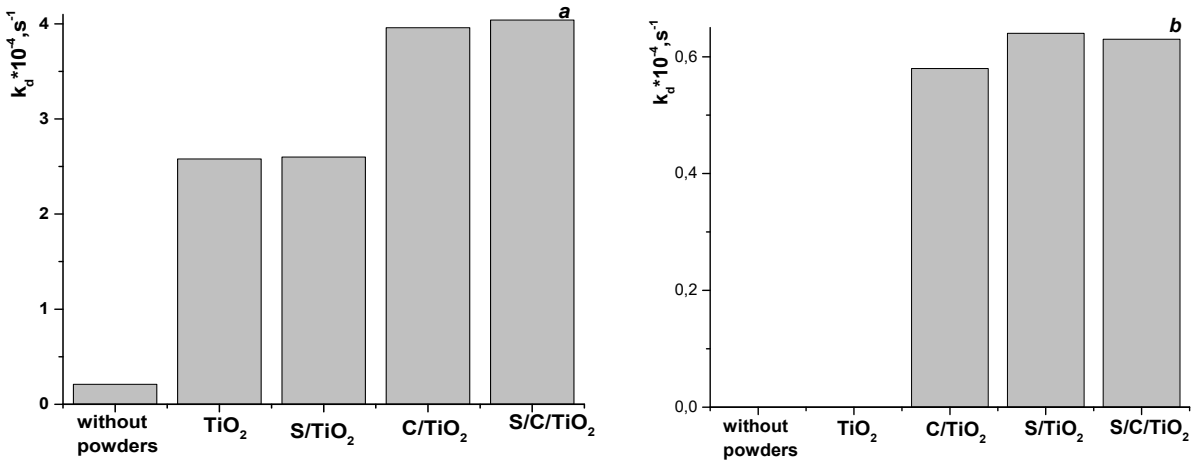

Fig. 7. The photocatalytic activity of nanocomposites in the destruction of safranine T under: *a* – UV irradiation; *b* – visible irradiation

In S-containing samples S(VI) ions can substitute Ti(IV) and form the Ti-O-S bonds, which allows us to modify the electronic structure of TiO_2 by displacing the electronic sites from O to S [31, 32]. The oxygen atom becomes a center that hinders the recombination of the electron-hole pairs under irradiation [33].

With the increasing of dopants amount the process rate is decreased due to high concentration of dopant acting as electron–hole recombination sites [12, 34] and hence photocatalytic activity is decreased.

To investigate the photocatalytic capability of the most active photocatalyst in repeated applications, five repetition cycles were performed. High activity of the photocatalyst in all the cases is observed up to the third cycle. After the fifth use, deactivation is noted that can be explained by blocking the active sites with the reaction products, which prevents photons from accessing active sites and reduces the number of radicals participating in photodestruction and by losses of the photocatalyst during the experiment. A similar effect was recorded in the paper [35].

Вплив модифікування діоксиду титану сіркою та вуглецем на його фізико-хімічні і фотокаталітичні властивості

М.В. Шаповалова, Т.А. Халявка, О.Ю. Хижун, Н.Д. Щербань, В.В. Пермяков, С.Н. Щербаков

Інститут сорбції та проблем ендоекології Національної академії наук України
вул. Генерала Наумова, 13, Київ, 03164, Україна, takhalyavka@ukr.net
Інститут проблем матеріалознавства ім. І.М. Францевича Національної академії наук України
вул. Кржижановського, 3, Київ, 03142, Україна
Інститут фізичної хімії ім. Л.В. Писаржевського Національної академії наук України
проспект Науки, 31, Київ, 03028, Україна
Інститут геологічних наук Національної академії наук України
вул. О. Гончара, 55б, Київ, 01054, Україна
Інститут ботаніки ім. М.Г. Холодного Національної академії наук України
вул. Терещенківська, 2, Київ, 01601, Україна

Отримано нанокомпозитні матеріали на основі TiO_2, доповані сіркою (S/TiO_2), вуглецем (C/TiO_2), вуглецем і сіркою ($S/C/TiO_2$). Порошки охарактеризовано методами РФА, РФЕС, BET, СЕМ, ЕДС, ТЕМ і УФ та видимою спектроскопією. За допомогою методів РФЕС та ЕДС показано, що порошок діоксиду титану містить тільки елементи Ti і O, композити C/TiO_2 містять елементи Ti, O, C, композити S/TiO_2 - Ti, O, S і композити $C/S/TiO_2$ – Ti, O, C і S.

Рентгенофазовий аналіз виявив наявність фази анатазу в усіх композитах, поява рутилу зафіксована лише зі збільшенням кількості сірки в сірковмісних порошках. Встановлено, що композити складаються з круглястих агломератів розмірами 5–30 мкм. Виявлено, що модифікування сіркою призводить до зменшення розміру часток діоксиду титану з 14 до 9–10 нм в композитах S/TiO_2, допування вуглецем призводить до збільшення розміру частинок від 14 до 19 нм, а одночасне модифікування діоксиду титану вуглецем і сіркою призводить до утворення частинок розміром 7–8 нм.

Аналіз ізотерм сорбції–десорбції азоту для всіх синтезованих зразків показав наявність петлі гістерезису, що свідчить про мезопористу структуру порошків. Ізотерми відповідають IV типу класифікації IUPAC для мезопористих матеріалів з формою петлі гістерезису H1 для C/TiO_2 та H2 для S/TiO_2 і $C/S/TiO_2$. Модифікування TiO_2 вуглецем та сіркою призводить до збільшення питомої поверхні (в 1.8 разів у випадку C/TiO_2, 3.3 рази для S/TiO_2 і 4.7 разів для $C/S/TiO_2$), об'єму пор і зменшення радіуса пор порівняно з TiO_2.

У спектрах поглинання нанокомпозитів спостерігається батохромний зсув у порівнянні зі смугою поглинання чистого діоксиду титану. Виявлено, що модифікування призводить до звуження ширини забороненої зони. Нанокомпозитні зразки виявили вищу фотокаталітичну активність у реакції деструкції сафраніну Т при УФ та видимому опроміненні порівняно з чистим TiO_2. Це може бути пов'язано з участю допантів в інгібуванні процесу рекомбінації електронів та дірок, продовженням часу життя зарядів, підвищенням ефективності міжфазового розподілу зарядів і формуванням додаткових електронних рівнів.

***Ключові слова**: нанокомпозити, діоксид титану, вуглець, сірка, сафранін Т, фотокаталітична активність*

Влияние модифицирования диоксида титана серой и углеродом на его физико-химические и фотокаталитические свойства

М.В. Шаповалова, Т.А. Халявка, О.Ю. Хижун, Н.Д. Щербань, В.В. Пермяков, С.Н. Щербаков

Институт сорбции и проблем эндоэкологии Национальной академии наук Украины
ул. Генерала Наумова, 13, Киев, 03164, Украина, takhalyavka@ukr.net
Институт проблем материаловедения им. И.Н. Францевича Национальной академии наук Украины
ул. Кржижановского, 3, Киев, 03142, Украина
Институт физической химии им. Л.В. Писаржевского Национальной академии наук Украины
проспект Науки, 31, Киев, 03028, Украина
Институт геологических наук Национальной академии наук Украины
ул. О. Гончара, 55б, Киев, 01054, Украина
Институт ботаники им. Н.Г. Холодного Национальной академии наук Украины
ул. Терещенковская, 2, Киев, 01601, Украина

Получены нанокомпозитные материалы на основе TiO_2, допированные серой (S/TiO_2), углеродом (C/TiO_2), углеродом и серой ($S/C/TiO_2$). Порошки были охарактеризованы методами РФА, РФЭС, БЭТ, СЭМ, ЭДС, ТЭМ, УФ и видимой спектроскопии. С помощью методов РФЭС и ЭДС показано, что порошок диоксида титана содержит только элементы Ti и O, композиты C/TiO_2 содержат Ti, O, C, композиты S/TiO_2 - Ti, O, S, и композиты $C/S/TiO_2$ - Ti, O, C и S.

Рентгенофазовый анализ показал наличие фазы анатаза во всех композитах, появление рутила зафиксировано только с увеличением количества серы в серосодержащих порошках. Установлено, что композиты состоят из агломератов округлой формы размерами около 5–30 мкм. Выявлено, что модифицирование серой приводит к уменьшению размера частиц диоксида титана с 14 до 9–10 нм в композитах S/TiO_2, допирование углеродом приводит к увеличению размера частиц с 14 до 19 нм, а одновременное модифицирование диоксида титана углеродом и серой приводит к образованию частиц размером 7–8 нм.

Анализ изотерм сорбции-десорбции азота для всех синтезированных образцов показал наличие петли гистерезиса, что свидетельствует о мезопористой структуре порошков. Изотермы соответствуют типу IV классификации IUPAC для мезопористых материалов с формой петли гистерезиса H1 для C/TiO_2 и H2 для S/TiO_2 и $C/S/TiO_2$. Модифицирование TiO_2 углеродом и серой приводит к увеличению удельной

поверхности (в 1.8 раза в случае C/TiO_2, 3.3 раза для S/TiO_2 и 4.7 раза для $C/S/TiO_2$), объема пор и уменьшению радиуса пор по сравнению с TiO_2.

В спектрах поглощения нанокомпозитов наблюдается батохромный сдвиг по сравнению со спектром чистого диоксида титана. Установлено, что модифицирование приводит к сужению ширины запрещенной зоны. Нанокомпозиты проявили более высокую фотокаталитическую активность в реакции деструкции сафранина Т под воздействием УФ и видимого облучения по сравнению с чистым TiO_2. Это может быть связано с участием допантов в ингибировании рекомбинации электронов и дырок, продлением времени жизни зарядов, увеличением эффективности межфазного разделения зарядов и формированием дополнительных электронных уровней.

***Ключевые слова**: нанокомпозиты, диоксид титана, углерод, сера, сафранин Т, фотокаталитическая активность*

REFERENCES

1. Barberio M., Barone P., Imbrogno A., Ruffolo S. A., La Russa M., Arcuri N., Xu F. Study of Dye Absorption in Carbon Nanotube-Titanium Dioxide Heterostructures. *J. Chem. Chem. Eng.* 2015. **9**(5): 245.
2. Chorna N., Smirnova N., Vorobets V., Kolbasov G., Linnik O. Nitrogen doped iron titanate films: photoelectrochemical, electrocatalytic, photocatalytic and structural features. *Appl. Surf. Sci.* 2019. **473**(15): 343.
3. Shestopal N., Linnik O., Smirnova N. Influence of metal and non-metal ions doping on the structural and photocatalytic properties of titania films. *Him. Fiz. Tehnol. Poverhni.* 2015. **6**(2): 203.
4. Park Y., Kim W., Park H., Tachikawa T., Majima T., Choi W. Carbon-doped TiO_2 photocatalyst synthesized without using an external carbon precursor and the visible light activity. *Appl. Catal. B*. 2009. **91**: 355.
5. Wang Sh., Zhao L., Bai L., Yan J., Jiang Q., Lian J. Enhancing photocatalytic activity of disorder engineered C/TiO_2 and TiO_2 nanoparticles. *J. Mater. Chem. A.* 2014. **2**: 7439.
6. Bondarenko M., Khalyavka T., Melnyk A., Camyshan S., Panasuk Ya. Paramagnetic and Photocatalytic Properties of C-S Co-Doped TiO_2 Nanocatalysts. *J. Nano- Electron. Phys*. 2018. **10**(6): 06039-1.
7. Ansón-Casaos A., Tacchini I., Unzue A., Martínez M. Combined modification of a TiO_2 photocatalyst with two different carbons forms. *Appl. Surf. Sci.* 2013. **270**: 675.
8. Lin C., Song Y., Cao L., Chen Sh. Effective photocatalysis of functional nanocomposites based on carbon and TiO_2 nanoparticles. *Nanoscale*. 2013. **5**(11): 4986.
9. Yuan L., Wei X., Martinez J.P., Yu C., Panahi N., Gan J.B., Zhang Y., Gan Y.X. Reaction Spinning Titanium Dioxide Particle-Coated Carbon Fiber for Photoelectric Energy Conversion. *Fibers*. 2019. **7**(5): 49.
10. Bondarenko M., Khalyavka T., Petrik I., Camyshan S. Photocatalytic activity of TiO_2-C nanocomposites in the oxidation of Safranin T under UV and visible light. *Theor. Exp. Chem*. 2018. **54**(1): 40.
11. Khalyavka T., Bondarenko M., Shcherban N., Petrik I., Melnik A. Effect of the C and S additives on structural, optical and photocatalytic properties of TiO_2. *Appl. Nanosci*. 2018. **8**(46): 1.
12. Lei X., Xue X., Yang H., Chen C., Li X., Pei J., Niu M., Yang Y., Gao X. Visible light-responded C, N and S co-doped anatase TiO_2 for photocatalytic reduction of Cr(VI). *J. Alloys Compd*. 2015. **646**: 541.
13. Yang G., Yan Z., Xiao T. Low-temperature solvothermal synthesis of visible-light-responsive S-doped TiO_2 nanocrystal. *Appl. Surf. Sci*. 2012. **258**(8): 4016.
14. Patent 1639892 SU. MKI, B22F9/02, 9/14 (Buleten No 16). Trikhleb V., Strelko V.V. Method of production of micro-, mesoporous carbon adsorbent. 2016. [in Ukrainian].
15. Rajagopal S., Nataraj D., Khyzhun O.Yu., Djaoued Y., Robichaud J., Senthil K., Mangalaraj D. Systematic synthesis and analysis of change in morphology, electronic structure and photoluminescence properties of pyrazine intercalated MoO_3 hybrid nanostructures. *Cryst. Eng. Comm*. 2011. **13**(7): 2358.
16. HenrichV.E., CoxP.A. *The Surface Science of Metal Oxides.* (Cambridge: Cambridge University Press, 1994).
17. Khyzhun O., Solonin Y., Dobrovolsky V. Electronic structure of hexagonal tungsten trioxide: XPS, XES, and XAS studies. *J. Alloys Compd*. 2001. **320**(1): 1.
18. Ivanov S., Barylyak A., Besaha K., Bund A., Bobitski Y., Wojnarowska-Nowak R., Yaremchuk I., Kus-Liśkiewicz M. Synthesis, Characterization, and Photocatalytic Properties of Sulfur- and Carbon-Codoped TiO_2 Nanoparticles. *Nanoscale. Res. Lett.* 2016. **11**(1): 140.

19. Rockafellow E., Stewart L., Jenks W.S. Is sulfur-doped TiO_2 an effective visible light photocatalyst for remediation? *Appl. Catal. B*. 2009. **91**: 554.
20. Colon G., Hidalgo M.C., Munuera G., Ferino I., Cutrufello M.G., Navio J.A. Cu-doped TiO_2 systems with improved photocatalytic activity. *Appl. Catal. B.* 2006. **67**(1–2): 41.
21. Yu J.C., Ho W., Yu J., Yip H., Wong P.K., Zhao J. Efficient Visible-Light-Induced Photocatalytic Disinfection on Sulfur-Doped Nanocrystalline Titania. *Environ. Sci. Technol*. 2005. **39**(4): 1175.
22. Ohno T., Akiyoshi M., Umebayashi T., Asai K., Mitsui T. Photocatalytic Activity of S-Doped TiO_2 Photocatalyst Under Visible Light. *Chem. Lett.* 2003. **32**(4): 364.
23. Wagner C.D., Riggs W.M., Davis L.E., Moulder J.F., Muilenberg G.E. *Handbook of X-ray Photoelectron Spectroscopy.* (Perkin-Elmer, Co., Minnesota, 1979).
24. Wu Z., Dong F., Zhao W., Wang H., Liu Y., Guan B. The fabrication and characterization of novel carbon doped TiO_2 nanotubes, nanowires and nanorods with high visible light photocatalytic activity. *Nanotechnol.* 2009. **20**(23): 235701.
25. Palanivelu K., Im J.S., Lee Y.-S. Carbon Doping of TiO_2 for Visible Light Photo Catalysis - A review. *Carbon Lett*. 2007. **8**(3): 214.
26. Peng W., Li H., Liu Y., Song S. Adsorption of methylene blue on graphene oxide prepared from amorphous graphite: Effects of pH and foreign ions. *J. Mol. Liq.* 2016. **221**: 82.
27. Bondarenko M.V., Khalyavka T.A., Shcherban N.D., Tsyba N.N. Mesoporous Nanocomposites Based on Titanium Dioxide and Carbon as Perspective Photocatalysts for Water Purification. *Nanosistemi, Nanomateriali, Nanotehnologii.* 2017. **15**(1): 99.
28. Gu D.E., Lu Y., Yang B.C., Hu Y.D. Facile preparation of micro-mesoporous carbon-doped TiO_2 photocatalysts with anatase crystalline walls under template-free condition. *Chem. Commun.* 2008. **21**: 2453.
29. Dubey P.K., Tripathi P., Tiwari R.S., Sinha A.S.K., Srivastava O.N. Synthesis of reduced graphene oxide–TiO_2 nanoparticle composite systems and its application in hydrogen production. *Int. J. Hydrogen Energy*. 2014. **39**(29): 16282.
30. Li X., Xiong R., Wei G. Preparation and photocatalytic activity of nanoglued Sn-doped TiO_2. *J. Hazard. Mater*. 2009. **164**(2–3): 587.
31. Devi L.G., Kavitha R. Enhanced photocatalytic activity of sulfur doped TiO_2 for the decomposition of phenol: a new insight into the bulk and surface modification. *Mater. Chem. Phys*. 2014. **143**(3): 1300.
32. Huang W.F., Chen H.T., Lin M.C. Density functional theory study of the adsorption and reaction of H_2S on TiO_2 rutile (110) and anatase (101) surfaces. *J. Phys. Chem. C*. 2009. **113**(47): 20411.
33. Zhang F., Wang M., Zhu X., Hong B., Wang W., Qi Z., Xie W., Ding J., Bao J., Sun S., Gao C. Effect of surface modification with H_2S and NH_3 on TiO_2 for adsorption and photocatalytic degradation of gaseous toluene. *Appl. Catal. B*. 2015. **170–171**: 215.
34. Fu X.L., Long J.L., Wang X.X., Leung D.Y.C., Ding Z.X., Wu L., Zhang Z.Z., Li Z.H., Fu X.Z. Photocatalytic reforming of biomass: A Systematic study of hydrogen evolution from glucose solution. *Int. J. Hydrogen Energy*. 2008. **33**(22): 6484.
35. Shaban Y.A., El Maradny A.A., Al Farawati R.Kh. Photocatalytic removal of polychlorinated biphenyls (PCBs) using carbon-modified titanium oxide nanoparticles. *Appl. Surf. Sci.* 2016. **328**: 114.

Received 18.07.2019, accepted 20.11.2019